IOP Conference Series:
Materials Science and
Engineering

PAPER · **OPEN ACCESS**

Structural modelling of multilayer skis with an open source FEM software

To cite this article: L Fraccaroli *et al* 2021 *IOP Conf. Ser.: Mater. Sci. Eng.* **1038** 012005

Structural modelling of multilayer skis with an open source FEM software

L Fraccaroli[1], C Gorla[2] and F Concli[1]

[1] Free University of Bolzano/Bozen, piazza Università 1, 39100 Bolzano, Italy
[2] Politecnico di Milano, via La Masa 1, 20157 Milano, Italy

e-mail: franco.concli@unibz.it

Abstract. The development process of mountaineering skis is characterized by a rapid design phase due to the continuous changes in materials, customer's requirements and manufacturing processes. Nowadays, this type of ski is still characterized by a design process based on a basilar trials and error technique. Finite Elements Analysis (FEA) could introduce a different approach to overcome main disadvantages, such as time, of this actual design method. For this reason, the main purpose of this work is centered on the development of a reliable FE model of an existing mountaineering ski, capable to forecast the mechanical behavior of the real tool. Firstly, all mechanical properties of materials that were composing the ski were characterized. Tensile tests in the two principal directions were performed on flat dog-bones shaped specimens. Secondly, Digital Image Correlation (DIC) was combined with results obtained from tensile tests in order to approximate the four in-plane (XY) elastic properties, namely, the two elastic modules, the shear module and the Poisson ratio (E_x, E_y, G_{xy}, ν_{xy}). Results of the cross-correlation process were after checked with the help of numerical simulations. FEA simulations were reproducing the tensile-tests configuration. Finally, geometry, mesh and simulations-run of the ski were performed in the open source environment Code_Aster/Salome-Meca. The results of simulations of the ski were compared with the response of the real ski in three-point bending tests. Differences of 2.5%-10% with respect to the real ski were observed for the different modelling techniques.

1. Introduction

Actually, the design process of ski mountaineering (skimo or skialp) is characterized by an important testing activity. Several prototypes are manufactured and verified with simple experimental mechanical tests for investigating principal properties, like torsional and bending stiffnesses. After that, for those that pass a first quality check, skis are tested by professional skiers that can give an important feedback on the ski behaviour under different practice conditions. Although this trial and error technique gives reliable results, it is evident that it has important limitations like the time necessary to the assembly process and costs of prototypes needed for the test phase. Reducing physical prototypes, with the help of numerical simulations (FEA), could be a relevant improvement in the design phase of this sport equipment. Finite Elements Analyses are already used in the development phase of downhill skis [1-4]. Several authors investigated the mechanical properties of alpine or carving skis [5-7]. However, this technology seems to be not yet used for the development phase of mountaineering skis. It was found that for ski mountaineering it is necessary to find a balance between performances and weight. This fact introduces an additional challenge in the design of the ski. The objective of this work was to create a numerical model of an existing ski developed from a leader manufacturing company. Skis were tested experimentally as well as materials that were composing them. Dog bones specimen were obtained starting from thin materials sheets, provided by the manufacturing company, thanks to laser cut technology. It must be pointed out that no standards were followed during the material characterization phase. The reason is related to the fact that material sheets provided did not respect the minimum geometry dimensions. Moreover, the aim of this initial phase was to extrapolate the two elastic modules in the two in-plane direction and not to prepare a detailed technical report. Digital image correlation [8-15] in combination with the Campbell formula [16] permitted the characterization of the four in plane elastic properties. Different levels of simplifications were introduced during simulations run. Finally, results of the numerical analysis were compared with the one obtained from the experimental test on the real ski, and, specifically, a three point bending tests[17,18].

2. Materials and methods

2.1. Ski overview

Skis are generally composed by a sandwich structure of composites materials, with a central softcore in wood or honeycomb that guaranties good flexibility and very low weight. The core is covered up with layers of composites materials like basalt, glass and carbon fibers reinforced constituents. These play a pivotal role for the resistance and stiffness of the sport equipment. In addition to structural layers, it is possible to find several materials that do not have mechanical purposes, like the top and the bottom boundary layers. The higher layer is used for improving the quality of decoration while the lower one is chosen for reducing the friction between the ski and the snow. A particular attention must be given to the correct choice between all components of the ski, a good balance between weight and downhill performances must be achieved. In this case the best solutions are the one with a high number of layers. Without the help of FEA the design process of a ski that has an increased level of constituents could be difficult and time consuming. In these cases, the experience of the manufacturer is the only available tool.

2.2. Material Characterization

Since the mechanical properties of materials that were composing the ski were not provided, the initial step of this work was dedicated to the characterization of the four in-plane elastic properties for each constituent. Fibers reinforced materials have two main constituents, fibers and matrix. Filaments take the major part of the load during operation while the matrix has to keep them together and protect them from external agents that can degrade them. For establishing mechanical properties, the theory of orthotropic laminas was taken into account. The material was considered having just one principal direction. Generally speaking, orthotropic materials can be described in 3D by means of 9 independent elastic constants, compared with the 21 required for a completely non isotropic material. For a lamina of small thickness and with longitudinal continuous fibers, the elastic behavior can be described by means of 4 independent elastic constants: the 2 in-plane elastic modules, the in-plane shear module and one of the two in-plane Poisson's ratios. In this work the two elastic modules were computed directly form the two different tensile tests while the Poisson's ratio was estimated thanks to the combined Tensile test-DIC approach. At last, the shear module was computed with the approximated Campbell formula[16].

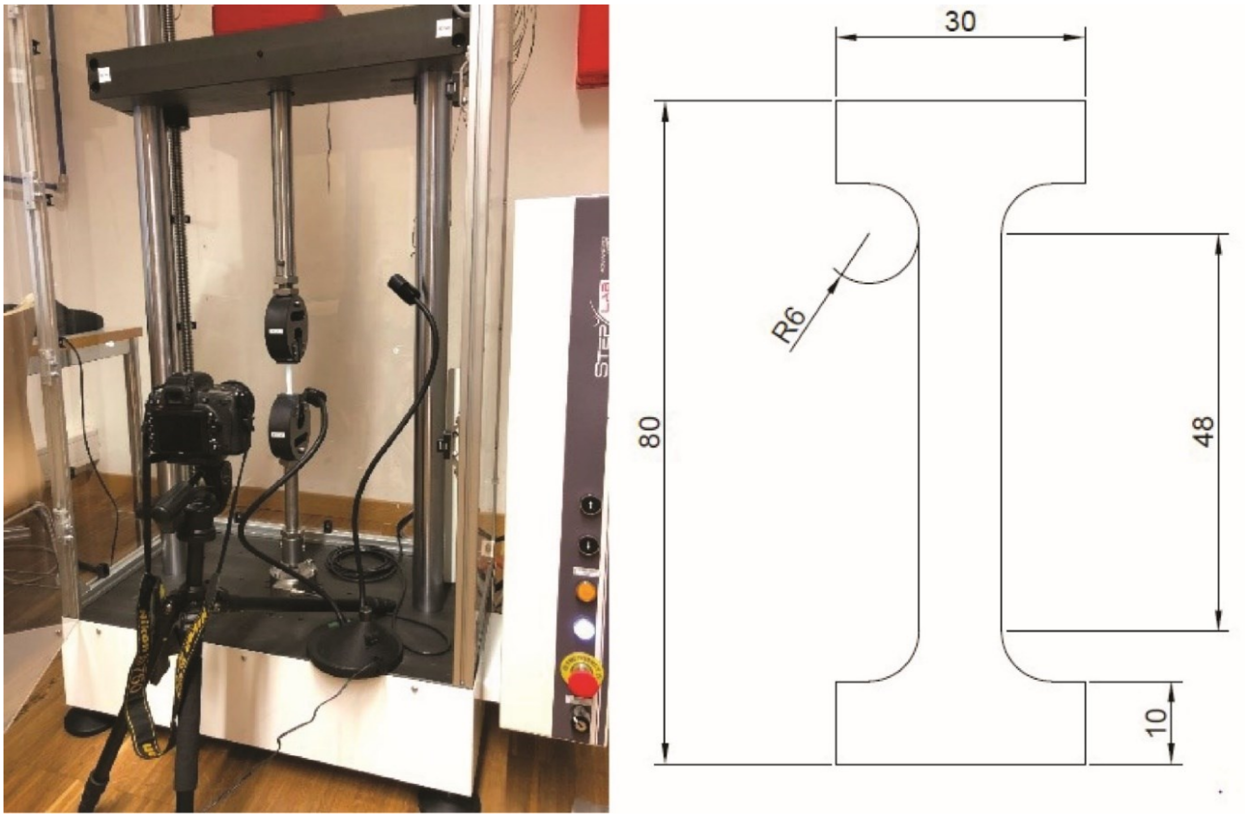

Figure 1. *STEPLab UD04 tensile machine and testing setup; (right) dog-bone sample geometry and dimensions.*

The provided materials sheets were divided with the help of a code number. Specifically, 9, 24, 139, 207, 290, 135, 31, 86 and 217. Monoaxial tests were performed on an STEPLab UD04 testing machine, visible in Figure 1, capable to apply static forces up to 4.5 kN. The tests were performed with a crosshead displacement velocity of 0.1 mm/min. The two elastic modules can be obtained from the two different tensile tests while the Poisson's ratio can be computed starting from strains in the two different directions (Eq.1).

$$\nu_{xy} = -\frac{\varepsilon_y}{\varepsilon_x} \quad ; \quad \nu_{yx} = -\frac{\varepsilon_x}{\varepsilon_y} \tag{1}$$

Another solution could be to use multiaxial strain gauges. However, the use of DIC represent a suitable solution. One camera (reflex Nikon D750 with a 24-85 zoom and a stabilizer), took pictures of the specimen at each timestep during the test. Moreover, the sample's surface is illuminated with an external constant light source.

2D Digital image correlation is an optical measurement approach used for reconstructing displacement and strain fields of a component that has a planar surface. This technique is based on the recognition of the gray scale, and, therefore, a characteristic "speckle" pattern (black and withe) must be applied on the surface of the tested specimen. In order to avoid out of plane deformation the camera must be positioned perfectly in a parallel plane with respect to the surface of the inspected part. Once the camera has been positioned, it acquires photos at a fixed rate during the whole tensile test. The first acquired picture takes the name of reference stage. On this first photo the post-processing algorithm creates a virtual grid, subdividing the total area into smallest surfaces called subsets or facets. Cross correlation operations allow the recognition of facets across timesteps (Figure 2). When subsets are recognized for each step, the algorithm reconstructs in order, displacement and strain fields. The software used is GOMrrelate [19].

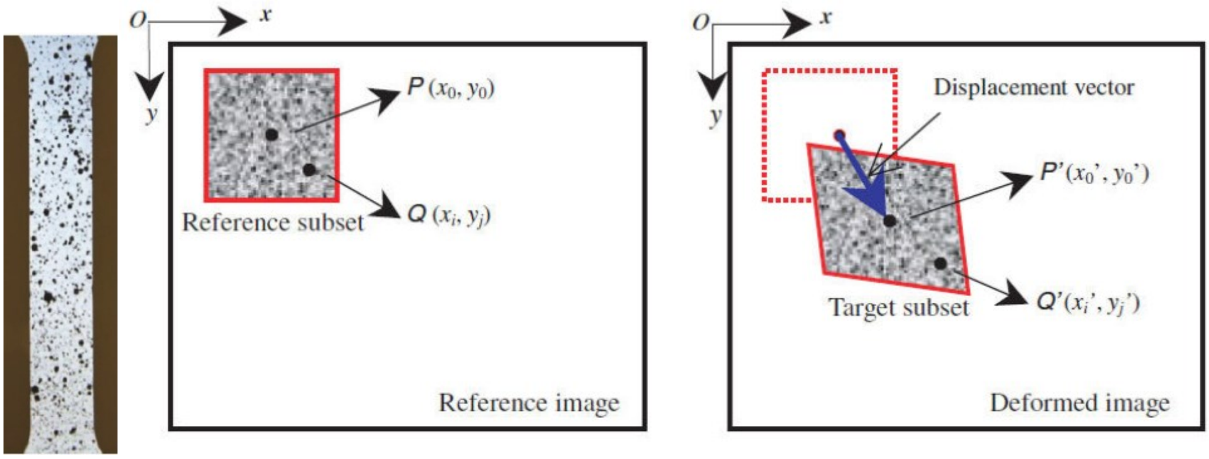

Figure 2. *DIC; (left) surface pattern; (right) cross correlation.*

Thanks to this technology it is possible to compute simultaneously the two strains into the two principal directions. With these data it is possible to use (Eq.1) to compute the Poisson's ratio. The shear module is after approximated thanks to the Campbell formula (Eq.2)

$$G_{xy} = \frac{E_x}{(1+\nu_{xy})} + \frac{E_y}{(1+\nu_{yx})} \tag{2}$$

2.3. FEA

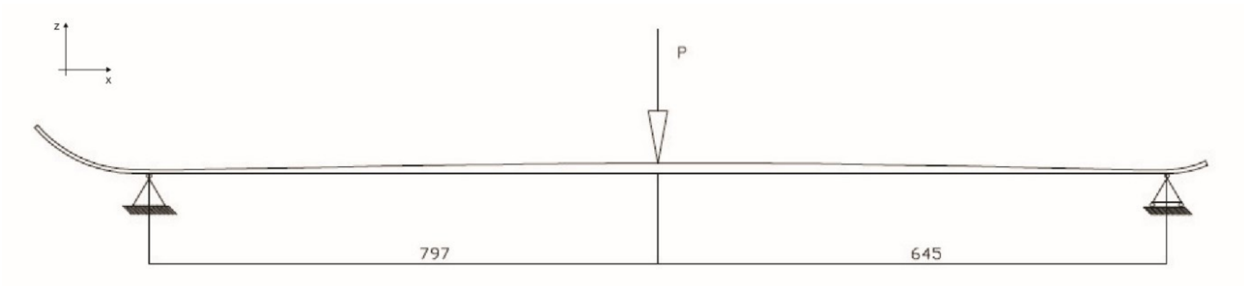

Figure 3. *Schematic representation of the three-point bending tests - reference case for the FE simulations.*

Two models with different levels of simplifications were tested.

2.3.1. Shell-model. During the modelling phase some simplifications were made. Firstly, the symmetry along the longitudinal plane of the ski was used. Therefore, only half component was geometrically reconstructed. Secondly, in order to replicate the three-point bending tests shown in Figure 3, only the part of the component between supports was simulated. Finally, due to their neglectable resistant contribution, also the steel edges were not insert into the modellization. Figure 4 shows the shell model of the ski. How it is possible to see, several subdivisions are present. They are needed for setting properly the height of the ski. The total length was subdivided into 145 smallest areas with a total number of 22382 quadrangular elements.

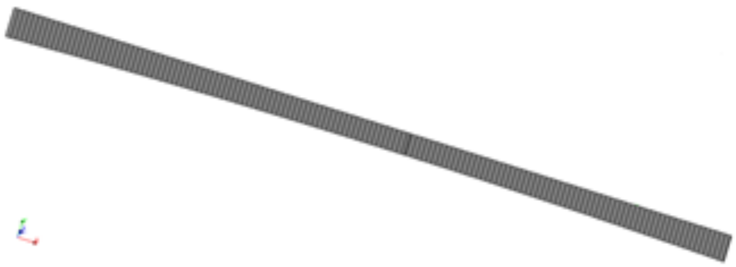

Figure 4. *Shell models used for the three-point-bending simulations.*

2.3.2. Solid-model The same modelling simplifications used for the 2D problem were also used for the solid analysis. Moreover, other considerations were made for defining correctly materials parameters. Indeed, 9 elastic constants are necessary to correctly describe fibers reinforced materials in 3D. According to [20], materials that are composed by only unidirectional long fibers have an equal elastic module in the two radial direction. Furthermore, due to thin laminas specimen, it was not possible to compute the shear module in out of plane directions. The poisson's ratio and shear modules found in the xy plane were set equal in each direction while the third elastic modules was set equal to the one in the y direction. On the other hand, as shown in Figure 5 and 6, in the solid model the lateral protective layer was also considered.

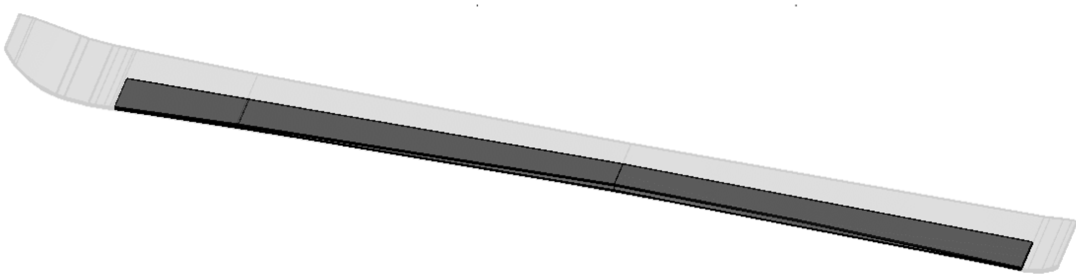

Figure 5. *Isometric view of the solid model used for the three-point-bending test.*

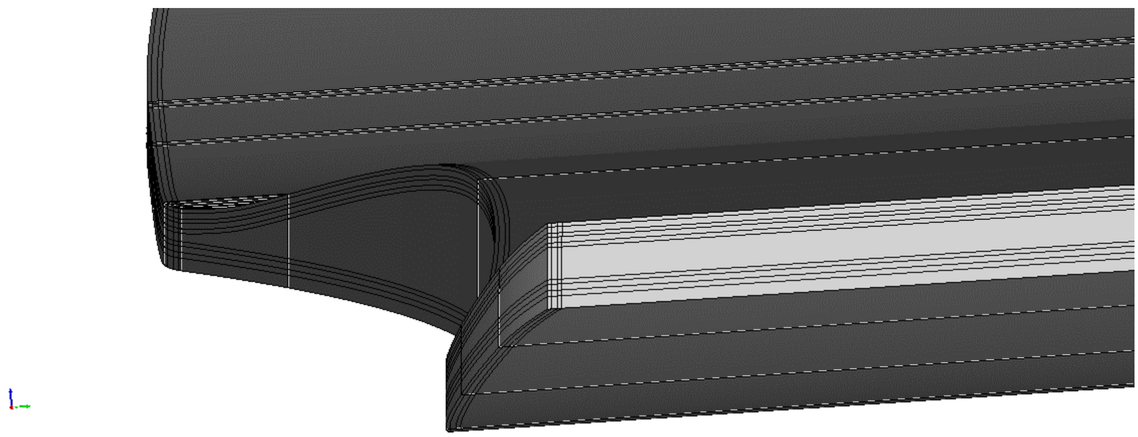

Figure 6. *Different layers of the solid model.*

IOP Conf. Series: Materials Science and Engineering 1038 (2021) 012005 doi:10.1088/1757-899X/1038/1/012005

In order to correctly compute the stress profile, the three-elements rule in the thickness was used for creating the mesh. The grid was made of quadratic hexahedrons only. A total number of about 500.000 elements mesh was created (for the simplified symmetric model used for the bending analysis)

3. Results

The results of the tensile tests in terms of stress strain curves are presented in from Figure 7 to Figure 13.

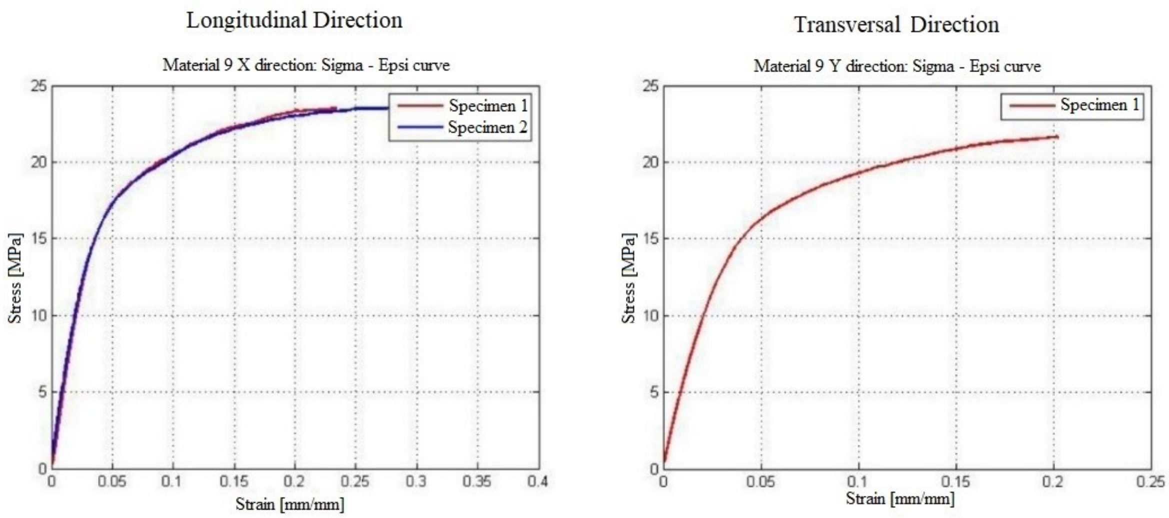

Figure 7. *Material 9 tensile tests.*

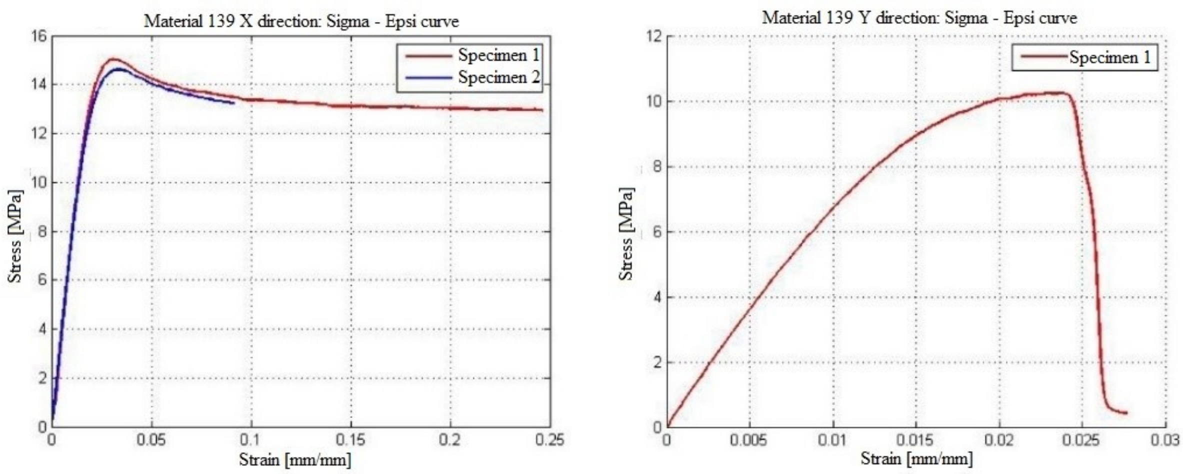

Figure 8. *Material 139 tensile tests.*

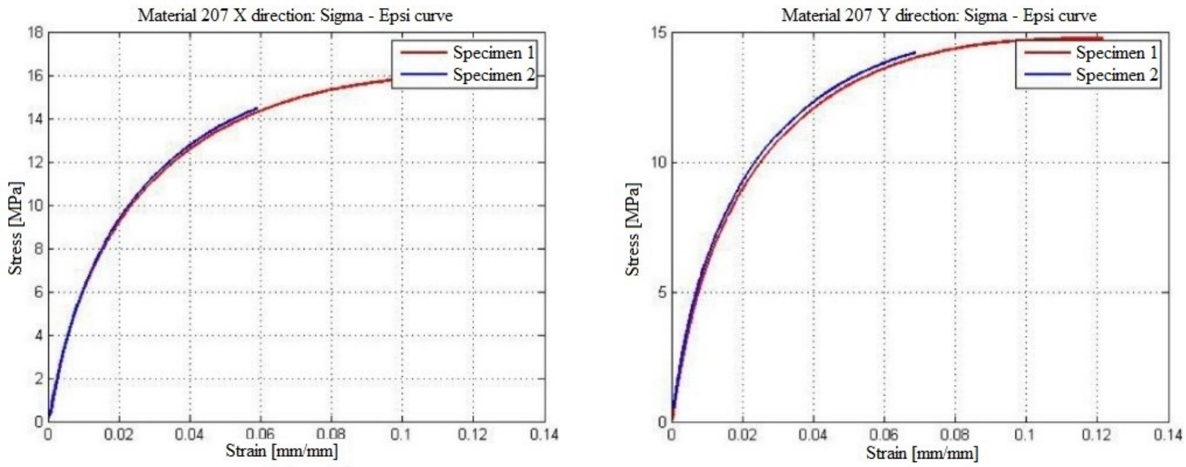

Figure 9. *Material 207 tensile tests.*

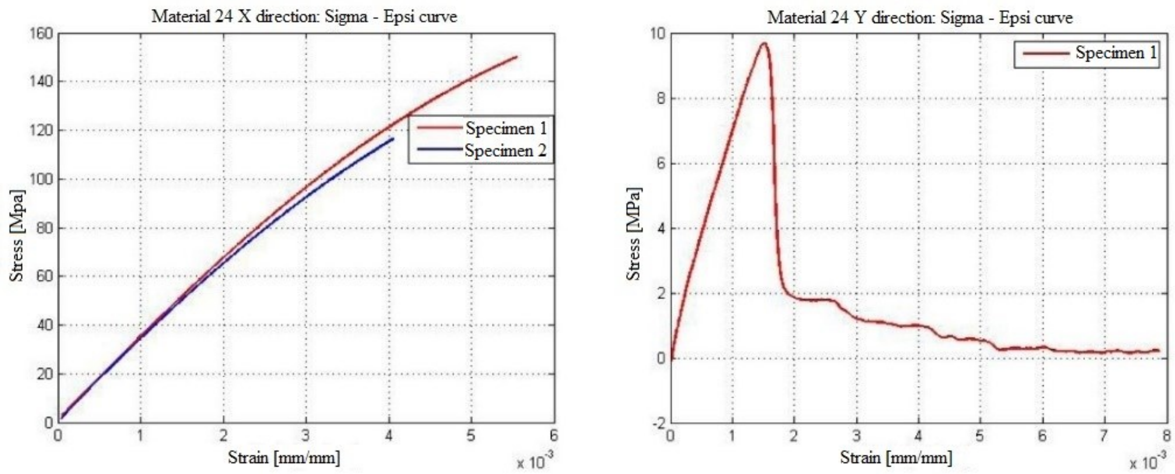

Figure 10. *Material 24 tensile tests.*

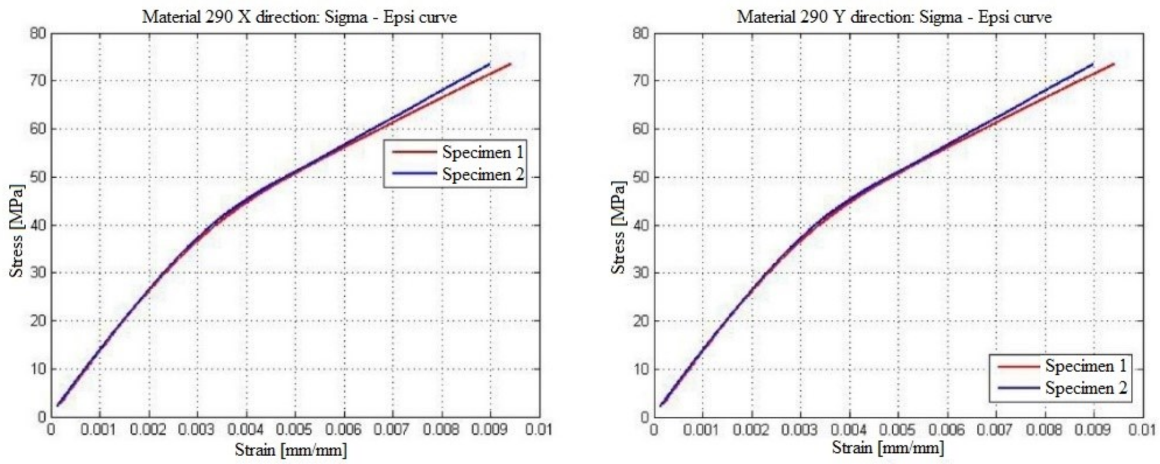

Figure 11. *Material 290 tensile tests.*

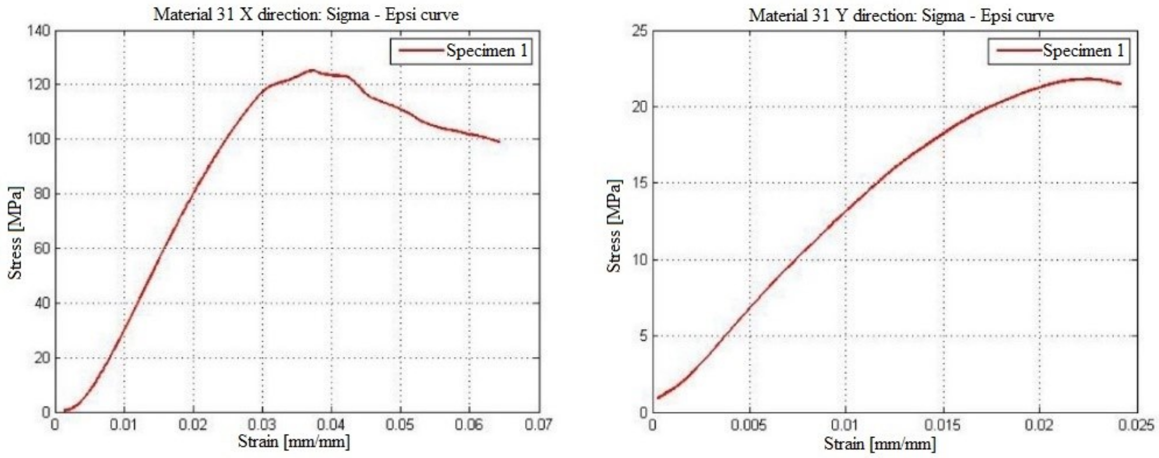

Figure 12. *Material 31 tensile tests.*

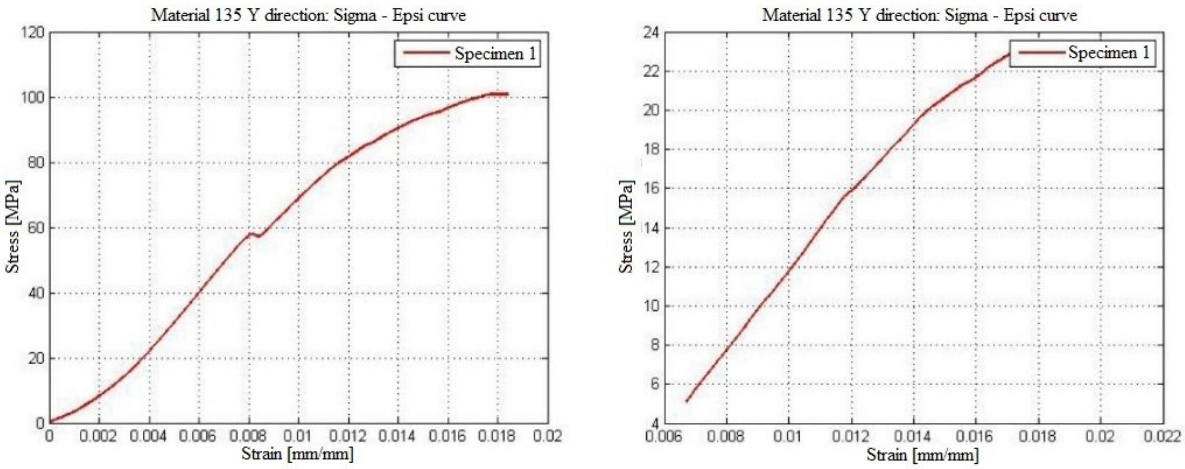

Figure 13. *Material 135 tensile tests.*

Table 1 shows the in-plane properties of the tested materials.

Table 1. *Material elastic properties.*

	Material								
	9	24	139	207	290	135	31	86	217
E_x [MPa]	550	35000	800	850	20000	4000	2000	13700	35000
E_y [MPa]	567	8700	750	897	13700	569	127	420	12436
v_{xy} [-]	0.45	0.23	0.45	0.42	0.18	0.39	0.39	0.40	0.56
v_{yx} [-]	0.43	0.35	0.38	0.30	0.12	0.39	0.39	0.40	0.48
G_{xy}[MPa]	776	35010	1097	1291	29125	3009	1184	10086	25327

Table 2 **s**hows displacements results of the ski in the point in which a load of 120N was applied. Tests were done thanks to 2 supports and a kettlebell for applying correctly the load. Two clamps ensured the ski to the supports and the kettlebell positioned in the middle of the ski through its handle. Results measured during the experimental tests were after compared to the one obtained with the two different numerical approaches.

Table 2. *Comparison of the maximum deflection of the ski in the three-point bending test: FEM vs. Experiments.*

Model	Displacement [mm]	Simulation time* [min]	Error [%]
Experimental	40		
Shell	41	35	2.5%
Solid	44	60	10.0%

*on a 9.6 GFLOPS workstation

Figure 14 reports the normal stresses in the point in which load was applied with respect to the thickness of the ski (0 corresponds to the bottom part).

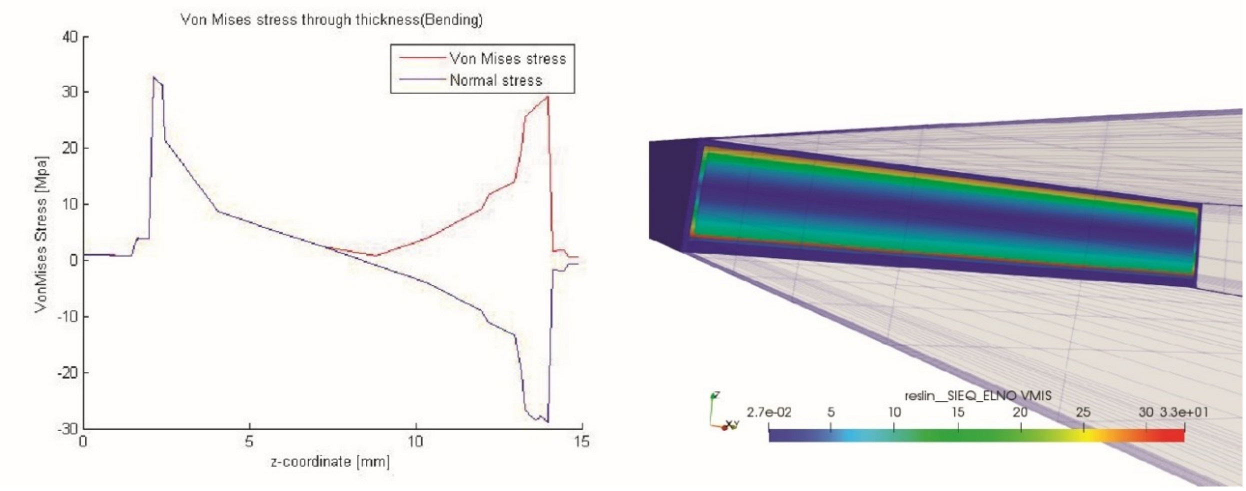

Figure 14. *Solid model results – three-point-bending test (normal and Von Mises stresses in the section).*

4. Discussion

Since the ski during operation must work within elastic field, only the linear part of the constitutive law was taken into account. The main part of the tested materials does not present differences in this initial part of interest. For materials #9 #24 and #139 no discrepancies were observed in the X directions. Due to low availability of materials, only one specimen was tested in the Y direction. For materials #207 and #290 it is possible to observe that no differences are present in both direction within the elastic field. Materials #31 and #135 were tested with different type of specimen, a rectangular probe was cut directly from the material sheet. For both of them the single fibers were easily visible. Tests on single materials will be object of future improvements, but in this initial phase of research, which is more focused on numerical simulations rather than on the exact characterization of the constituents of the ski, the collected data seem sufficient.

Numerical simulations highlight a good match with the experimental measurements for both of the modelling approaches. For the shell FEM model (three-point bending) a displacement of 41mm with an error of 2.5% with respect to the experimental results was observed. The 3D simulations present a maximum displacement of 44mm with a 10% corresponding error. For the shell model, discrepancies in the predicted displacement/rotation with respect to the measured one can be attributed to the following reasons:

- The ski is modelled with small rectangles that have different heights thus, the perfect curved shape of the ski was not correctly replicated.

- The steel edges and the lateral layers (cage) were neglected.

On the other side, comparing the solid model with the experimental test, it is possible to give some motivation for the higher discrepancy including:

- The longitudinal curvature of the ski was not considered.
- The assumption on the material properties taken during material characterization affected results.

The lateral cage influenced also the discrepancies between the solid and the shell model. Both have the same width, and the lateral areas were present only in the 3D simulation. Since these lateral areas have a lower resistant contribution, it is acceptable that the solid model has a higher deflection. Looking from figure 7 to 13 it is possible to say that not all materials have structural purposes, in fact, some materials were chosen for other reasons. For example, the bottom material is used for reducing the friction with the snow in order to improve in operation performances. FEA allows an accurate evaluation on how each layer is contributing to the total stiffness of the ski.

5. Conclusions

An exact numerical model capable to describe the behaviour of a real ski is hard to achieve. However, in this research a 2.5%-10% error approximation was reached. A key step that influenced hugely the model replication was the material characterization phase. It was not possible to follow standards for tensile tests due to material dimensions problems. This fact must be considered during the results evaluation. However, a good level of approximation was reached. Moreover, the use of DIC was mandatory for correctly describe the materials. Comparing results of the three-point bending with their relative numerical simulations, better results were achieved with the shell approach. With a maximum error of 2.5% for the pure bending test. For the solid approach a 10% error was reached. The fact that the 2D problem presents minor errors is due to lower levels of approximations used.

Once the model is verified, it can be possible to easily change materials and layer configurations in order to observe different ski behaviours. This fact leads to a huge reduction of costs and time needed for the development phase of the component, specifically for the prototyping and testing phase. Future improvements will be a more accurate modelling of the ski without simplification in terms of material properties. The fact that steel edges were not modelled, influenced securely the performance of the ski.

It must be noticed that during operation the ski is subjected to much more complex load conditions. The loads applied depends on the ski deflection and how the snow deforms. Moreover, properties of the snow itself like temperature, mechanical and thermal cycles experienced, humidity, etc. can influence the ski performance.

Due to this aspect, the validation of the simulation under real load conditions is very difficult to achieve. A contact FEM model with the snow should be considered and validated experimentally with on snow tests. This step will be investigated in the next phase of the research. In conclusion it should be highlighted that while the results achieved are not perfectly reproducing the real ski performance, the accuracy is satisfactory considering all the simplifications and hypothesis introduced.

References

[1] Wolfsperger F, Szabo D and Rhyner H 2016 Development of Alpine Skis Using FE Simulations *Procedia Eng.* **147** 366–71
[2] Federolf P, Roos M, Lüthi A and Dual J 2010 Finite element simulation of the ski-snow interaction of an alpine ski in a carved turn *Sport. Eng.* **12** 123–33
[3] ZBONCAK R 2018 Experimental Verification of Ski Model for Finite Element Analysis *56*

Conf. experimetnal Stress Anal. 450–6

[4] Mössner M, Innerhofer G, Schindelwig K, Kaps P, Schretter H and Nachbauer W 2013 Measurement of mechanical properties of snow for simulation of skiing *J. Glaciol.* **59** 1170–8

[5] Nordt A A . G S S L P K 1999 Computing the mechanical properties of alpine skis *Sport. Eng.* **2** 65

[6] Hirano Y and Tada N 1994 Mechanics of a turning snow ski *Int. J. Mech. Sci.* **36** 421–9

[7] Cresseri S and Jommi C 2005 Snow as an elastic viscoplastic bonded continuum: a modelling approach *Ital. Geotech.* **4** 43–58

[8] Musotto Z 2012 *" Digital Digital Image Correlation : Correlation applicazione di tecniche convenzionali e sviluppo di soluzioni la stima e l ' incremento dell ' accuratezza*

[9] Crammond G, Boyd S W and Dulieu-Barton J M 2013 Speckle pattern quality assessment for digital image correlation *Opt. Lasers Eng.* **51** 1368–78

[10] Makeev A, He Y, Carpentier P and Shonkwiler B 2012 A method for measurement of multiple constitutive properties for composite materials *Compos. Part A Appl. Sci. Manuf.* **43** 2199–210

[11] Kowalczyk P 2019 Identification of mechanical parameters of composites in tensile tests using mixed numerical-experimental method *Meas. J. Int. Meas. Confed.* **135** 131–7

[12] Schreier H W and Sutton M A Systematic Errors in Digital Image Correlation Due to Undermatched Subset Shape Functions 303–10

[13] Wattrisse B, Chrysochoos A and Muracciole J 2000 Analysis of Strain Localization during Tensile Tests by Digital Image Correlation 29–39

[14] W. P W . R 1982 Digital image techniques in experimental stress analysis *Opt. Eng.* **21** 427–31

[15] Górszczyk J, Malicki K and Zych T 2019 Application of Digital Image Correlation (DIC) Method for Road Material Testing *Materials (Basel).* **12** 2349

[16] Yokoyama T and Nakai K 2007 Evaluation of in-plane orthotopic elastic constants of paper and paperboard *Proc. SEM Annu. Conf. Expo. Exp. Appl. Mech. 2007* **3** 1505–11

[17] Fraccaroli L *Structural modelling of multilayer skis* (Free University of Bolzano/Bozen)

[18] Fraccaroli L and Concli F 2020 Introduction of Open-Source Engineering Tools for the Structural Modeling of a Multilayer Mountaineering Ski under Operation *Appl. Sci.* **10** 5310

[19] Anon www.gom.com

[20] Aerospaziali T E M CAPITOLO 32 - Materiali compositi: la legge costitutiva ortotropa